MATEC Web of Conferences **21**, 06002 (2015)
DOI: 10.1051/matecconf/20152106002

Wrinkling behavior in tube hydroforming coupled with internal and external pressure

X.L. Cui[1], X.S. Wang[1,2,a], and S.J. Yuan[1,2]

[1] School of Materials Science and Engineering, Harbin Institute of Technology, 150001 Harbin, China
[2] National Key Laboratory of Precision Hot Processing of Metals, Harbin Institute of Technology, 150001 Harbin, China

Abstract. Control and use of wrinkles is a challenge in tube hydroforming because wrinkle was always considered as one of the defects of tubes from the traditional view. In this paper, a dedicated experimental setup was designed and manufactured, using which the investigation of wrinkling behavior coupled with internal and external pressure can be realized. The effect of internal or external pressure on 5A02 aluminum alloy tubes and 0Cr18Ni9 stainless steel tubes were all investigated using this setup. It was found that the number and shape of wrinkles are strongly dependent on the internal or external pressure. More important is that the geometrical configuration of wrinkles can be perfectly characterized using the Gauss function rather than the sine function adopted in the published literature. In addition, the fitted Gauss functions for every wrinkle were integrated in order to compare their area with the corresponding area of die cavity, so as to obtain the appropriate process parameters for the useful wrinkle, which can be formed in advance and then flatted in the calibration stage.

1. Introduction

In the past few years, tube hydroforming technology has attracted considerable attention for the fabrication of lightweight hollow-structure components. During hydroforming, three major modes of failure, i.e. bursting, localized wrinkling and global buckling, may take place on the tubes. Either wrinkling or buckling of tubes can be caused by excessive axial compressive stress due to axial feeding [1, 2]. Wrinkle was always considered as one of the defects of tubes in the past investigations, which must be avoided as far as possible [3–6]. However, it is believed by Yuan et al. [7] that not all wrinkles are defects and that the concept that some wrinkles can be controlled and used in tube hydroforming was proposed to improve the formability of tubes. The "useful" wrinkles should be formed in advance to accumulate materials in the expansion zone, and then they can be flattened in the subsequent calibration stage. Therefore, the shape and dimensions of the wrinkles should be controlled according to the optimal relationship between the internal pressure and axial feeding. In the previous attempting the wrinkles are assumed that distributed in the die cavity evenly and the wave

[a] Corresponding author: hitxswang@hit.edu.cn

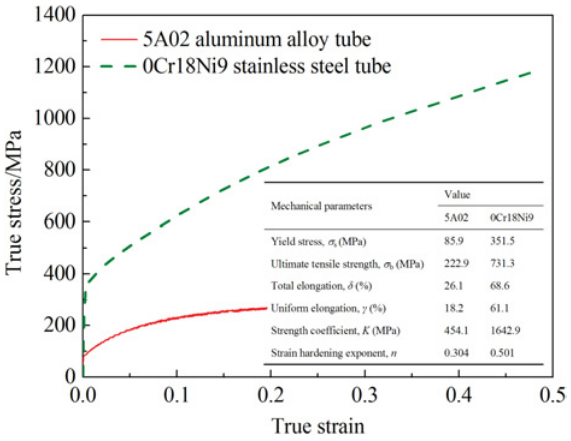

Figure 1. True stress-strain curves of as-received tube materials along the axial direction.

shape of the wrinkle is described by a sine curve [7]. However, only the wave top of the wrinkle can be accurately described by a sine curve which is invalid for the wave bottom. It is imperative that a more suitable function should be selected to fit the whole wrinkle for the further analysis of wrinkle shape and dimensions quantitatively.

As far as the wrinkling behavior in tube hydroforming was concerned, Yuan et al. [8–10] conducted many experimental and numerical analyses of wrinkling behavior in tube hydroforming. However, the wrinkling behavior of thin-walled tubes is mainly induced by the axial compression or internal pressure/axial compression, and is just a preliminary study which needs further exploration with the update of equipment technology. When the internal pressure and external pressure are introduced to both inner and outer surfaces of the tube simultaneously, the stress state applied on the tube cannot be simplified as plane stress state. It is therefore necessary to investigate experimentally whether the wrinkling behavior has a dependence on the external pressure.

In this paper, in order to conduct further research on the wrinkling behavior of tubes under internal pressure, and to carry out a preliminary study on the coupled effect of internal and external pressure, a dedicated experimental setup was developed. The effects of internal and external pressure on the wrinkling behavior of 5A02-O aluminum alloy tubes and 0Cr18Ni9 stainless steel tubes were investigated.

2. Preparations

2.1 Materials

The as-received tube materials used in this study are 5A02 aluminum alloy tube and 0Cr18Ni9 stainless steel tube with outer diameter of 63 mm and nominal thickness of 2 mm. The 5A02 aluminum alloy tube was drawn from extruded tube and then annealed at 380° for approximately 2 h, while the 0Cr18Ni9 stainless steel tube was commercial stainless steel seamless tubes for fluid transport. The uniaxial tensile tests were conducted on an Instron 5569 machine along the axial direction of the two tubes respectively. The true stress-strain curves are shown in Fig. 1.

2.2 Experimental setup and precedence

A dedicated experimental setup for the investigation of wrinkling behavior was designed and manufactured, as shown in Fig. 2. To carry out an experimental investigation of the wrinkling behavior

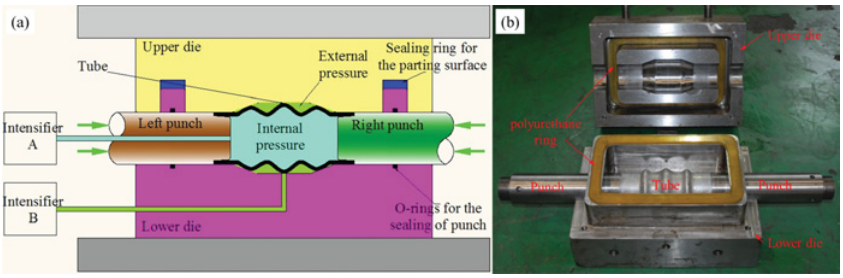

Figure 2. Experimental setup: (a) schematic diagram of experimental setup; (b) experimental die.

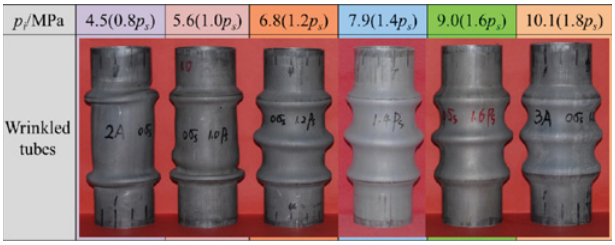

Figure 3. Wrinkled tubes under different internal pressures.

of tubes coupled with internal and external pressure, the experimental die, varies from the conventional hydroforming die with a flat parting surface, has been designed into embedded structure in order to guarantee the sealing of external pressure by the polyurethane ring embedded into the space between upper and lower die. The working components of the experimental die are the upper die, lower die, left punch and right punch.

The wrinkling investigations were carried out on the upgraded 20 MN hydroforming press at Harbin Institute of Technology. In this investigation, the tube had a total length of 210 mm, and both punches were advanced to a maximum stroke of 15 mm in all experiments, i.e. a total axial feeding of 30 mm. Moreover, different internal pressures of 1.2p_s, 1.4p_s, 1.6p_s and 1.8p_s were used to investigated the effect of internal pressure. When the wrinkling behavior coupled with internal and external pressures was concerned, three cases which were constant pressure difference, constant internal pressure and increasing internal pressure respectively, were used in this paper.

3. Results and discussion

3.1 Effect of internal pressure on the wrinkling behavior

Figure 3 shows the wrinkled tubes under different internal pressures with a total punch stroke of 30 mm. It can be found from Fig. 3 that the wrinkles only occur at both ends of the deformation zone when the internal pressure was lower (0.8 p_s) and the two wrinkles are distorted and non-axisymmetric. When the internal pressure was increased to 1.0p_s, the wrinkles on both sides of the tube change into an axisymmetric pattern. Meanwhile, another wrinkle, called middle wrinkle, starts to develop between the two previous wrinkles. For the cases with higher internal pressure (1.2p_s, 1.4p_s, 1.6p_s and 1.8p_s), three axisymmetric wrinkles were formed. One small difference is that the bigger diameter wrinkle occurs in the middle of the tube. In addition, the wrinkles became fatter with increasing internal pressure.

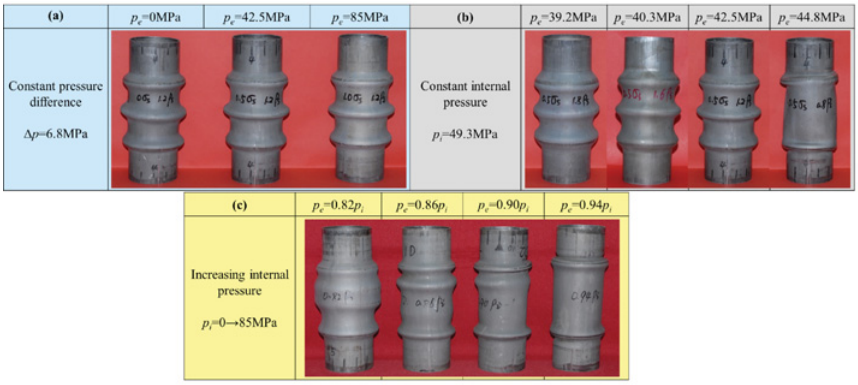

Figure 4. Effect of external pressure on the wrinkling behavior: (a) constant pressure difference; (b) constant internal pressure; (c) increasing internal pressure.

3.2 Effect of external pressure on the wrinkling behavior

Figure 4 shows the wrinkled tubes coupled with internal and external pressure in order to reveal the effect of external pressure on the wrinkling behavior from three cases. It is shown that the wrinkling behavior has hardly any dependence on the external pressure for the case of constant pressure difference, which is attributed to the similar distribution trend of stresses regardless of applied external pressure. In contrast, the formation of a middle wrinkle could be prevented by higher external pressure both for the case of constant internal pressure and the case of increasing internal pressure. However, the shape and dimensions of wrinkles exhibits large differences between these two cases, as shown in Fig. 4(b) and (c).

3.3 Geometrical analysis of wrinkles wave

It can be seen in Fig. 3 that the wave shape, especially for the middle wrinkle, is more likely to be fitted using the GaussAmp function, which is shown as follows:

$$y = y_0 + Ae^{-\frac{(x-x_c)^2}{2w^2}} \tag{1}$$

where y_0 can be used to represent the radius of the wave bottom, A is the amplitude and can be used to represent the height of the wrinkle, x_c is the axial coordinate of the wave top, and w is a parameter that is related to the full width at half maximum and can be represent the degree of fatness of the wrinkle.

Figure 5 shows the experimental data and fitted curves of wrinkles using Eq. (1) for internal pressures of $1.2p_s$, $1.4p_s$, $1.6p_s$ and $1.8p_s$, respectively. It can be clearly seen in Fig. 5 that the wrinkles can be fitted perfectly using the GaussAmp function, especially for the middle wrinkles. Moreover, the fitted functions for every wrinkle under different internal pressures have been given in Table 1.

3.4 Wrinkling behavior of different tube materials

The wrinkling behaviour of 5A02 and 0Cr18Ni9 tube was compared experimentally when the internal pressure was 1.2 p_s, as shown in Fig. 6(a). Then the experimental data and the corresponding fitted curves of the wrinkles were all shown in Fig. 6(b). It can be seen clearly that both the wrinkles of 5A02 and 0Cr18Ni9 tube can be fitted accurately using the GaussAmp function. The wrinkles of 0Cr18Ni9 tube is fatter than that of 5A02 tube, while the radius of the wave bottom for the 0Cr18Ni9 tube is bigger

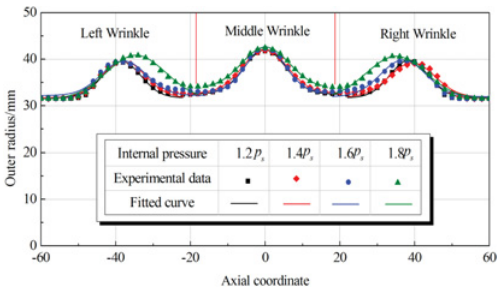

Figure 5. Fitted curves of wrinkles using the GaussAmp function.

Table 1. Fitted functions for the wrinkles under different internal pressures.

	Left wrinkle	Middle wrinkle	Right wrinkle
$1.2p_s$	$y = 31.679 + 7.818\exp\left[-\frac{(x+38.356)^2}{53.018}\right]$	$y = 32.454 + 9.540\exp\left[-\frac{(x+0.038)^2}{62.612}\right]$	$y = 31.672 + 8.082\exp\left[-\frac{(x-38.495)^2}{52.547}\right]$
$1.4p_s$	$y = 31.689 + 7.930\exp\left[-\frac{(x+37.839)^2}{66.691}\right]$	$y = 32.672 + 9.439\exp\left[-\frac{(x+0.074)^2}{71.080}\right]$	$y = 31.790 + 7.418\exp\left[-\frac{(x-39.376)^2}{74.964}\right]$
$1.6p_s$	$y = 32.163 + 7.445\exp\left[-\frac{(x+37.815)^2}{73.079}\right]$	$y = 32.814 + 9.849\exp\left[-\frac{(x-0.087)^2}{53.392}\right]$	$y = 31.900 + 7.909\exp\left[-\frac{(x-36.955)^2}{75.567}\right]$
$1.8p_s$	$y = 31.342 + 9.486\exp\left[-\frac{(x+34.544)^2}{127.665}\right]$	$y = 33.812 + 8.782\exp\left[-\frac{(x-0.083)^2}{80.682}\right]$	$y = 31.495 + 9.120\exp\left[-\frac{(x-35.063)^2}{128.026}\right]$

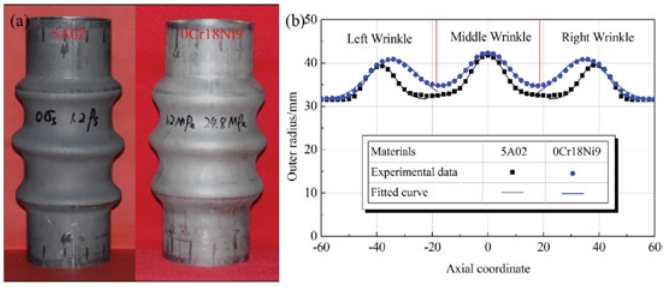

Figure 6. Comparison of wrinkling behavior between 5A02 and 0Cr18Ni9 tube: (a) wrinkled tubes; (b) fitted curves.

than that of the 5A02 tube. Moreover, the distance between two wrinkles is shorter for the 0Cr18Ni9 tube. All the results mentioned above indicate that the wrinkle resistance of 5A02 aluminum alloy tube is relatively weaker than that of the 0Cr18Ni9 tube. When the wrinkles occur on the 5A02 aluminum alloy tube the wrinkling instability will favour a sustained deterioration in the local area. On the contrary, the hardening of 0Cr18Ni9 tube due to wrinkling will transfer the wrinkling instability to the undeformed area.

3.5 Flattening of wrinkles during calibration stage

The wrinkled tubes under different internal pressures were hydroformed with the same calibration pressure of 80MPa in order to investigate the effect of wrinkling behaviour on the formability, as shown in Fig. 7. When the internal pressure during wrinkling stage is low ($0.8p_s$ and $1.0p_s$), the tube fractures before making contact with the die in the calibration stage due to the lack of sufficient materials in the middle of the tube. With the increasing internal pressure during wrinkling stage, the wrinkled tubes cannot be flatted completely; as a result the dead wrinkles appear on the

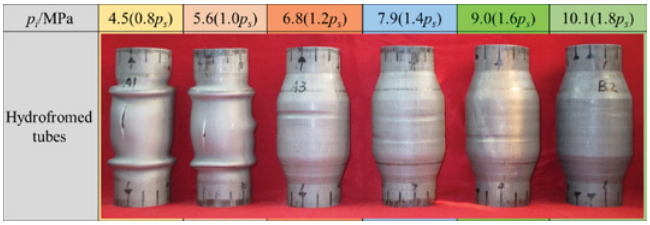

Figure 7. Hydroformed results of wrinkled tubes.

Table 2. Comparison of surface area of single wrinkle wave and that of the corresponding die cavity.

	Surface area of left wrinkle/mm^2			Surface area of middle wrinkle/mm^2			Surface area of right wrinkle/mm^2		
	S_{die}	$S_{wrinkle}$	$S_{wrinkle}$-S_{die}	S_{die}	$S_{wrinkle}$	$S_{wrinkle}$-S_{die}	S_{die}	$S_{wrinkle}$	$S_{wrinkle}$-S_{die}
1.2p_s	10014	9585	-429	11750	11281	-469	10014	9674	-340
1.4p_s	10548	10006	-542	10681	10474	-207	10548	9868	-680
1.6p_s	11082	10791	-291	9613	9894	280	11082	10458	-624
1.8p_s	11082	10813	-268	9613	9695	82	11082	10743	-339

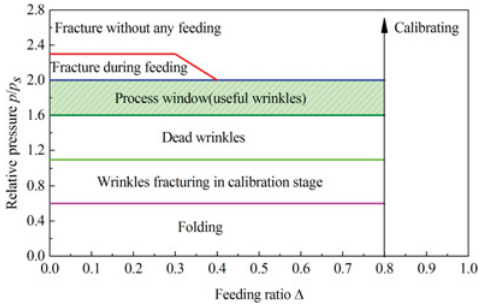

Figure 8. Schematic diagram of process window diagram for tube hydroforming.

hydroformed tubes. Higher wrinkling internal pressure will alleviate the occurrence of dead wrinkles. Therefore, a well-hydroformed tubular specimen can be obtained with a wrinkling internal pressure of 1.8 p_s.

It is well known that the surface area of single wrinkle wave can be obtained based on Eq. (1)

$$S = 2\pi \int_{x_1}^{x_2} \left(y_0 + Ae^{-\frac{(x-x_c)^2}{2w^2}} \right) \sqrt{1 + \frac{A^2 (x - x_c)^2}{w^4} e^{-\frac{(x-x_c)^2}{w^2}}} dx. \tag{2}$$

The analytical solution cannot be given from this definite integral; however, the value of S can be obtained by numerical integration method in MATLAB, which have been listed in Table 2. It can be found that the smaller the difference between surface area of wrinkle and die ($S_{wrinkle}$–S_{die}) is, the easier the wrinkles can be flatted in the calibration stage.

From the discussion above, a process window diagram for tube hydroforming could be established, as shown in Fig. 8. In the process window diagram the wrinkling internal pressure and the axial feeding amount have been normalized and the useful wrinkles can be preformed to obtain the well-hydroformed tubes based on the process window diagram.

4. Conclusions

In this paper, the wrinkling behaviour of tube hydroforming coupled with internal and external pressure was investigated using a dedicated experimental setup. In a word, the wrinkling behaviors, such as the number and shape of wrinkles have a strong dependence on the internal pressure and the coupled effect of internal and external pressure.

Furthermore, wrinkles wave can be fitted perfectly using the GaussAmp function when the internal pressure is $1.2p_s$, $1.4p_s$, $1.6p_s$ and $1.8p_s$, respectively, and the fitting functions for the wrinkles can be used to predict the shape and dimensions of the wrinkles, the relative positions between two wrinkles and the effect of process parameters on the shape and dimensions of the wrinkles. It is more important that the fitted functions for the wrinkles can be integrated numerically in order to compare their area with the corresponding area of die cavity, so as to obtain the appropriate process parameters for the useful wrinkle. At the end, the wrinkled tubes were hydroformed and a normalized process window diagram for tube hydroforming was established.

References

[1] F. Dohmann, Ch, Hartl, J Mater Process Tech **60**, 669 (1996)
[2] N. Asnafi, Thin Wall Struct **34**, 295 (1999)
[3] S. Kim, Y. Kim, J Mater Process Tech **128**, 232 (2002)
[4] G. Nefussi, A. Combescure, Int J Mech Sci **44**, 899 (2002)
[5] E. Chu, Y. Xu, Int J Mech Sci **46**, 263 (2004)
[6] E. Chu, Y. Xu, Int J Mech Sci **46**, 285 (2004)
[7] S. Yuan, X. Wang, G. Liu, Z.R. Wang, J Mater Process Tech **182**, 6 (2007)
[8] L. Lang, S. Yuan, X. Wang, Z.R. Wang, Z. Fu, J. Danckert, K.B. Nielsen, J Mater Process Tech **146**, 377 (2004)
[9] S. Yuan, W. Yuan, X. Wang, J Mater Process Tech **177**, 668 (2006)
[10] L. Lang, H. Li, S. Yuan, J. Danckert, K.B. Nielsen, J Mater Process Tech **209**, 2553 (2009)